Characterization of three tissue fractions in corn (Zea mays) cob

AUTHOR(S):

Takada, Masatsugu; Niu, Rui; Minami, Eiji; Saka, Shiro

CITATION:

Takada, Masatsugu ...[et al]. Characterization of three tissue fractions in corn (Zea mays) cob. Biomass and Bioenergy 2018, 115: 130-135

ISSUE DATE:

2018-08

URL:

http://hdl.handle.net/2433/259771

Title

Characterization of three tissue fractions in corn (*Zea mays*) cob

Authors

Masatsugu Takada, Rui Niu, Eiji Minami, Shiro Saka*

Department of Socio-environmental Energy Science, Graduate School of Energy Science, Kyoto University, Yoshida-honmachi, Sakyo-ku, Kyoto 806-8501, Japan

* Corresponding author. E-mail: saka@energy.kyoto-u.ac.jp

Keywords

microscopic observation; cinnamic acids; hemicellulose; lignin; tissue fractions

Abstract

Corn (*Zea mays*) cob is composed of three tissue fractions: chaff (21.1%), woody ring (77.5%) and pith (1.4%). In this study, the cell wall components in these tissue fractions were characterized so as to examine their tissue morphology. As a result, it was found that the chemical compositions in three fractions were relatively similar, and the hemicellulose was the main component. Through their sugar composition analysis, hemicellulose was mainly composed of xylan in all fractions, while the proportion of arabinose and galactose was different in the woody ring, compared with other two fractions. From the alkaline nitrobenzene oxidation analysis, lignin in all fractions was composed all of guiacyl, syringyl and *p*-hydroxyphenyl lignins, while their ratios varied in three fractions. Furthermore, the amounts of cinnamic acids such as ferulic and *p*-coumaric acids, which are associated with the corn lignin, were also different among three fractions. With respect to the tissue morphology, the component cells in three fractions were totally different each other. Furthermore, from the ultraviolet microspectrophotometry of each morphological region in three tissue fractions, it was found that the lignin concentration and distribution

of cinnamic acids were different from one morphological region to another. These kinds of information would provide a clue as to efficient utilization of corn cob into value-added chemicals.

1. Introduction

Corn (*Zea mays*) is the most produced foodstuff in the world like the sugarcane [1]. As a by-product of the corn production, corn cob is estimated to be produced with the yield of 164 million Mg all over the world [2]. For its utilization, various researches have been conducted to produce valuable chemicals such as xylitol [3,4], ethanol [3,5–10] and cellulose nanofibers [11–13]. For the practical production, corn cob has been used as a resource for bioethanol production in China since 2013 [14]. In order to utilize the lignocellulosics for biofuels or chemicals, it is quite essential to understand its chemical characteristics and structures.

The cell walls of the lignocellulosics are mainly composed of cellulose, hemicellulose and lignin, and their components and compositions are different depending on the lignocellulosic species [15]. For the whole corn cob, several researchers have studied its chemical structures, especially for hemicellulose [9,16,17]. On the other hand, the corn cob is composed of three tissue fractions: chaff, woody ring and pith [18]. The shapes, densities and physical structures are totally different among the three fractions,

while their detailed chemical structures were not characterized yet.

In this study, thus, the chemical compositions and the characteristics of the main cell wall components such as cellulose, hemicellulose and lignin, were examined for the separated three tissue fractions of the corn cob. Furthermore, their component cells and the distributions of lignin including cinnamic acids were examined with ultraviolet microspectrophotometry.

2. Materials and methods

2.1. Samples and chemicals

Corn used in this study was harvested in Langfang city, Habei province, China. The sampling time and sample age were April 2015 and 0.4 years, respectively. The storage temperature and humidity before delivery to the laboratory were 10-20°C and 60-70%, respectively. The sample condition during delivery was air-dried and the corn cob was separated from grans before the delivery. These information was shown in accordance with the checklist for sample definition by Barton [19].Upon arrival in the laboratory, three different tissue fractions (outer part, chaff; middle part, woody ring; inner part, pith) were separated by using a knife as shown in Fig. 1, and the separated fractions were dried at 105°C for 12 h to measure their oven-dried weight. The fractionated samples were then milled in a small grinder (Wonder Blender WB-1: Osaka chemical Co., Ltd., Osaka, Japan), and used for various analyses. The analyses described below were conducted at least 3 times and the average values were used. The chemicals used in this study were of

reagent grade without any purification, purchased from Nacalai Tescque, Inc., Kyoto, Japan. The unit "%" used in this paper is based on weight.

---(Fig. 1)---

2.2. Analytical methods

Chemical compositions in three tissue fractions were evaluated using the method of Rabemanolontsoa et al. [20].

X-ray diffractograms were obtained by Rigaku RINT 2,200V (Rigaku Corp., Tokyo, Japan) with Ni-filtered Cu-Kα radiation (λ = 0.1542 nm) generated at 40 kV and 30 mA to evaluate the crystalline structure of cellulose, according to the ordinary method for holocellulose production [21]. The crystallinity index is estimated according to the calculation methods by Segal et al. as shown below [22].

$$\text{Crystallinity index (CrI)} = \frac{I_{002} - I_{am}}{I_{002}} \times 100$$

92

93 I_{002} is the maximum intensity of the 002 lattice diffraction at 2θ = 22.5°, and I_{am} is the

94 intensity of the diffraction at 2θ = 18.0°.

95

96 The composition of hemicellulosic saccharides was determined using the acid

97 methanolysis method [23], and the obtained monosaccharides were quantified by gas

98 chromatography-mass spectrometry (GC-MS) analysis using GCMS-QP 2010 Ultra

99 (Shimadzu Co., Kyoto, Japan) after the trimethylsilyl derivatization [2]. Furthermore,

100 acetic acid content was analyzed using the acid hydrolysis method with 72% H_2SO_4

101 followed by 3% H_2SO_4 [24]. Subsequently, the obtained hydrolyzates were analyzed with

102 high performance liquid chromatography (HPLC) (LC-10A, Shimadzu Co., Kyoto,

103 Japan) [2].

104 For the analysis of the lignin structure, the alkaline nitrobenzene oxidation was

105 performed according to the ordinary method and the total yields of vanillin,

106 syringaldehyde, and *p*-hydroxybenzaldehyde were determined by gas chromatography

107 (GC: GC 2014, Shimadzu Co., Kyoto, Japan) [25]. The vanillin and *p*-

hydroxybenzaldehyde can be produced from ferulic acid and *p*-coumaric acid, respectively, since both acids were associated with corn lignin [26–30]. Thus, the yields of cinnamic acids-derived vanillin and *p*-hydroxybenzaldehyde were subtracted from the original yield of the alkaline nitrobenzene oxidation products to obtain the actual yields of products from lignin.

As described above, the corn lignin contained some cinnamic acids such as ferulic acid (4-hydroxy-3-methoxycinnamic acid) and *p*-coumaric acid (4-hydroxycinnamic acid). The fractionated flour was treated with 0.5 mol L^{-1} NaOH to extract the cinnamic acids [31]. The extracted portion was acidified with dilute HCl and then extracted with ethyl acetate. The ethyl acetate-soluble portion was then dehydrated and evaporated under vacuum. The obtained products were trimethylsilyl derivatized followed by GC-MS analysis [32].

2.3. Microscopic observations

The distribution of lignin including cinnamic acids were observed by UV microscopy [33]. Each tissue fraction was embedded in epoxy resin, and the samples were cut into 0.5 μm thick section with a diamond knife mounted on a Leica Reichert Supernova Microtome (Buffalo Grove, IL, USA). The sections were placed on the quartz slides, mounted with glycerin and covered with quartz coverslip before examination by MSP-800 system (Carl Zeiss, Oberkochem, Germary) with a specified filter at 280 nm ± 5 nm. The morphological regions of the each fraction were analyzed on a UV microspectrophotometry based on photometric point-by-point measurements (spot size: 1 μm × 1 μm).

3. Results and discussions

3.1. Characteristics and chemical compositions of three tissue fractions

The images of three tissue fractions of corn cob and their dried weight compositions are shown in Fig. 1. The corn cob is composed of three tissue fractions whose physical structures are different one another. The outer part, chaff, is light and stiff, and its structure is wrinkled. The middle part, woody ring, is a lignified structure and very stiff like a woody xylem. The inner part, pith, is extremely light and its structure is spongy. The chaff, woody ring and pith account for 21.1%, 77.5% and 1.4%, respectively.

The chemical compositions in three tissue fractions are presented in Table 1. Hemicellulose is the main component in all fractions, especially in the woody ring with 46.9%. Cellulose is the second largest component, next to the hemicellulose, and the proportion of the holocellulose (cellulose + hemicellulose) is quite high in all regions. On the other hand, the lignin content is less than 20% in all fractions, smaller than that of woody biomass. Although the woody ring sounds to be high in lignin content, its content is, in fact, lower than other two fractions. For the extractives, the pith contained 3.5%, which is the highest among three fractions. The ash content is the highest in the chaff and the lowest in the woody ring. Accordingly, there are some differences in the chemical composition between three tissue fractions, while their overall compositions are relatively

similar. Since each component was quantified independently, the total values are not necessary equal to 100%. However, it was not adjusted.

For the further characterization, the detailed analyses of the main cell wall components such as cellulose, hemicellulose and lignin were conducted for three fractions.

---(Table 1)---

3.2. Structure of each cell wall component of three tissue fractions

3.2.1. Cellulose

In order to examine the crystalline structure of cellulose in three fractions, X-ray diffractometric (XRD) analysis was performed and Fig. 2 shows the X-ray diffractograms of the holocellulose (cellulose + hemicellulose) obtained from three morphological regions. Their XRD patterns are relatively similar. The XRD intensity of the pith is lower than those of other two fractions, due perhaps to its quite low density. The crystallinity

171 indexes of their holocelluloses are calculated according to the methods of Segal et al. and
172 shown in Fig. 2. As a result, the crystallinity index of holocellulose from woody ring
173 (42.4) is the highest, compared with those of chaff (39.9) and pith (38.5), but their
174 crystallinity indexes are quite similar, indicating that their structures of crystalline
175 cellulose are relatively similar.

176 ---(Fig. 2)---

177

178

179 3.2.2. Hemicellulose

180

181 The hemicellulosic sugar compositions in three tissue fractions are presented in Table 2.
182 Xylose is the main sugar components in all fractions. Among three fractions, the woody
183 ring contained higher proportion of xylose, while its arabinose and galactose contents are
184 much lower compared to the chaff and pith. As to the uronic acids, both glucuronic acid
185 and 4-*O*-methyl glucuronic acid are obtained from the chaff and pith, while for woody
186 ring, 4-*O*-methyl glucuronic acid was not detected. Accordingly, the hemicellulosic sugar

components are the same in three fractions except for 4-*O*-methyl glucuronic acid, whereas their sugar compositions are different among three fractions.

In addition, the acetic acid, which is considered to be derived from the acetyl residue, are obtained from all fractions. Their yields in chaff, woody ring and pith are 2.8%, 4.7% and 4.4%, respectively.

---(Table 2)---

3.2.3. Lignin

For the structural analysis of lignin, the alkaline nitrobenzene oxidation was performed for three tissue fractions, and the results are shown in Fig. 3. As the decomposed products from guaiacyl (G), syringyl (S) and *p*-hydroxyphenyl (H) lignins, vanillin, syringaldehyde and *p*-hydroxybenzaldehyde are obtained, respectively. In case of the corn lignin, the cinnamic acids such as ferulic acid and *p*-coumaric acid are associated with lignin as described above. By the alkaline nitrobenzene oxidation, the ferulic acid and *p*-

203 coumaric acid can be converted into the vanillin and *p*-hydroxybenzaldehyde,
204 respectively. Thus, the yields of the decomposed products from lignin were evaluated
205 from the total yields of decomposed products minus the yields of decomposed products
206 from cinnamic acids. As a result, all of three decomposed products were obtained from
207 all tissue fractions, indicating that lignin in three fractions are composed all of G, S and
208 H lignins. The yields of the decomposed products are highest in the woody ring and the
209 lowest in the chaff. For all fractions, vanillin is the main products, while the ratios of
210 syringaldehyde and *p*-hydroxybenzaldehyde are different among three fractions,
211 indicating that the compositions of G, S and H lignins would be different from one tissue
212 fraction to another.

213 ---(Fig. 3)---

214 Table 3 shows the yields of ferulic acid and *p*-coumric acid in three tissue fractions
215 as determined by the aqueous alkali treatment. As a result, both yields are different in
216 three tissue fractions. The content of ferulic acid in the woody ring is lower than that in
217 the chaff and pith. In herbaceous plants, ferulic acid is associated with lignin and
218 hemicellulose via ester and ether linkages as bridges between lignin and hemicellulose,

219 forming lignin/phenolics - carbohydrate complexes (LCC) [34], and the ferulic acid
220 esterified the *O*-5 position of α-L-arabinofuranosyl residues of arabinoxylan [26–29]. Fig.
221 4 shows the correlation between ferulic acid and arabinose contents in three tissue
222 fractions. The woody ring, whose ferulic acid content is the lowest, contains the lowest
223 arabinose content among three fractions. The positive correlation between ferulic acid
224 and arabinose contents would be due to the LCC linkages between them. It is interesting
225 that the woody ring contains high hemicellulose content, while low arabinose and ferulic
226 acid contents, indicating that the woody ring would contain less LCC structure compared
227 to other fractions.

228 ---(Table 3)---

229 ---(Fig. 4)---

230 With respect to the *p*-coumaric acid, in case of the corn stover, the *p*-coumaric acid
231 is associated with S lignin at γ position of propane side-chain according to the 2D-NMR
232 analysis [30]. Fig. 5 shows the correlation between the *p*-coumaric acid content and
233 syringaldehyde obtained by alkaline nitrobenzene oxidation in three tissue fractions.
234 Given that the syringaldehyde is obtained from S lignin, its yield can be an indicator to

evaluate the ratio of S lignin. As a result, woody ring, whose *p*-coumaric acid content is the highest, produces the highest yields of syringaldehyde compared to other fractions. Accordingly, the *p*-coumaric acid might associate with S lignin as well as corn stover. However, further experiments should be required to discuss the detailed chemical structures.

---(Fig. 5)---

3.3. UV microscopy of three tissue fractions

Fig. 6 shows the ultraviolet (UV) micrographs of three tissue fractions taken at a wavelength of 280 nm. Among the cell wall components, only lignin can absorb UV light due to its aromatic structure. Thus, the darker area in UV micrographs shows the higher concentration of lignin to be blacker. The three tissue fractions are composed of different types of cells.

---(Fig. 6)---

The chaff is composed of sclerenchyma cells and their structures are wrinkled (Fig. 6 (a)). The middle lamella portion shows blacker compared to the cell wall portion, indicating that the lignin concentration in the middle lamella would be higher than that in the cell wall.

The woody ring is composed of vascular bundle and parenchyma cells as shown in Fig. 6 (b-1) and (b-2), respectively. The vascular bundle region is composed of various kinds of cells such as fiber, vessel and sieve tube. Compared to the parenchyma region, the vascular bundle region shows blacker, which indicates that the lignin concentration of vascular bundle region would be higher than that of parenchyma region. As well as the chaff, the middle lamella portion is higher in its lignin concentration compared to the cell wall portion.

Regarding the pith (Fig. 6 (c)), the size of component cell is quite large with an average diameter of 100 μm and all of them are parenchyma cells. Air spaces are often observed between the adjacent cells.

For more detailed analysis of the lignin distribution in the three tissue fractions, the UV microspectrophotometry was performed for each morphological region, and the

267 results are shown in Fig. 7. As for the sclerenchyma cells in chaff (Fig. 7 (a)), the cell
268 wall (CW) and the middle lamella at cell corner (ML_{CC}) shows the highest peak at a
269 wavelength of 323 nm and 318 nm, respectively. In case of the ordinary woody biomass,
270 both the secondary wall and the middle lamella show the peak at a wavelength of 275~280
271 nm [35,36]. According to the experiments with the model compounds, it was found that
272 the ethyl-ferulate and ethyl-*p*-coumarate showed the peak at a wavelength of 325 nm and
273 313 nm, respectively [37]. Thus, it would be more likely that the shift of peak wavelength
274 from 280 nm to 320 nm is due to the association of cinnamic acids to corn lignin.
275 Accordingly, the difference in the wavelength of peak between CW and ML_{CC} would
276 indicate that the CW contains more ferulic acid compared to *p*-coumaric acid, while ML_{CC}
277 contains more *p*-coumaric acid compared to ferulic acid. Therefore, the distribution of
278 cinnamic acids would be different from one morphological region to another.

279 ---(Fig. 7)---

280 For the woody ring, the UV spectra of the vessel, the sieve tube, the fiber and the
281 parenchyma are shown in Fig. 7 (b-1, b-2). Since the cell walls of fiber and parenchyma
282 have enough thickness to determine the UV spectra (1 μm × 1 μm), their CW and ML_{CC}

283 regions were separately determined. All spectra showed the peak at a wavelength of
284 around 320 nm as well as those of chaff. The UV spectra of vessel and parenchyma
285 showed the highest absorbance at 315 nm, while those of fiber showed at 325 nm for both
286 CW and ML_{CC} potions. Such results would indicate that the fiber contained more ferulic
287 acid compared to *p*-coumaric acid, while the vessel and parenchyma contained more *p*-
288 coumaric acid.

289 For the pith, UV microspectrophotometry analysis was performed not for each
290 morphological region, since the cell wall and middle lamella can not be distinguished due
291 to the thin cell wall and there are no ML_{CC} due to the air spaces. As a result, the highest
292 UV absorbance was obtained at a wavelength of 320 nm as well as other two fractions.

293 From the UV spectrophotometric analysis, it was found that cinnamic acids are
294 not uniformly distributed in three tissue fractions and their distributions are different from
295 one morphological region to another. However, further experiments would be required to
296 discuss the quantitative evaluation of the distribution of lignin including cinnamic acids.

297

Conclusions

The characterization of chemical structures was performed for three tissue fractions of corn (*Zea mays*) cob; chaff, woody ring and pith. As a result, the chemical compositions in three fractions were relatively similar, and the hemicellulose was the main component in all fractions. With respect to the hemicellulosic sugar, the woody ring contained higher xylose and lower of arabinose and galactose compared to chaff and pith. From the alkaline nitrobenzene oxidation, the compositions of G, S and H lignins would be different from one tissue fraction to another. As for the cinnamic acids, the woody ring contained lower furulic acid and higher of *p*-coumaric acid compared to other fractions. The ferulic acid content has a positive correlation with arabinose content, and *p*-coumaric acid with syringaldehyde yields by nitrobzene oxidation. These positive correlations would indicate their chemical structures in corn cob.

From the UV microspectrophotometry analysis, the component cells were totally different in three tissue fractions and the lignin concentration and the distribution of cinnamic acids were different from one morphological region to another.

314 The differences of chemical composition and lignin structures in lignocellulosics
315 influence on its decomposition behaviors in various kind of treatments. Furthermore, the
316 distribution of lignin also has an impact on the delignification behaviors. Accordingly,
317 these results obtained in this study are quite important to understand the decomposition
318 behaviors of corn cob in various decomposition treatments. Thus, such information would
319 provide a clue as to efficient utilization of corn cob for biofuels or biochemicals.
320
321
322
323 **Acknowledgements**
324
325 This work was supported by the Japan Science and Technology Agency (JST) under the
326 Advanced Low Carbon Technology Research and Development Program (ALCA) and
327 Kakenhi (No. 16J11212) a Grant-in-Aid for Japan Society for the Promotion of Science
328 (JSPS) fellow, for which the authors are extremely grateful.
329

330 **References**

331

332 [1] World Agricultural Production, Production, supply and distribution, 2016.
333 http://apps.fas.usda.gov/psdonline/

334 [2] M. Takada, R. Niu, E. Minami, S. Saka, Two-step hydrolysis of corn (*Zea mays*)
335 cobs treated with semi-flow hot-compressed water, Int. J. Agric. Crop Sci. (2017).
336 (in press)

337 [3] F. Latif, M.I. Rajoka, Production of ethanol and xylitol from corn cobs by yeasts
338 Bioresource Technology, Bioresour. Technol. 77 (2001) 57–63.

339 [4] H. Ling, K. Cheng, J. Ge, W. Ping, Statistical optimization of xylitol production
340 from corncob hemicellulose hydrolysate by *Candida tropicalis* HDY-02, N.
341 Biotechnol. 28 (2011) 673–678.

342 [5] D.S. Beall, L.O. Ingram, A. Ben-Bassat, J.B. Doran, D.E. Fowler, R.G. Hall, B.E.
343 Wood, Conversion of hydrolysates of corn cobs and hulls into ethanol by
344 recombinant *Escherichia coli* B containing integrated genes for ethanol production,
345 Biotechnol. Lett. 14 (1992) 857–862.

346 [6] H.G. Lawford, J.D. Rousseau, Fuel ethanol from corn residue prehydrolysate by a
347 patented ethanologenic *Escherichia coli* B, Biotechnol. Lett. 14 (1992) 421–426.
348 [7] M. Chen, L. Xia, P. Xue, Enzymatic hydrolysis of corncob and ethanol production
349 from cellulosic hydrolysate, Int. Biodeterior. Biodegrad. 59 (2007) 85–89.
350 [8] K. Liu, X. Lin, J. Yue, X. Li, X. Fang, M. Zhu, J. Lin, Y. Qu, L. Xiao, High
351 concentration ethanol production from corncob residues by fed-batch strategy,
352 Bioresour. Technol. 101 (2010) 4952–4958.
353 [9] D. Van Eylen, F. van Dongen, M. Kabel, J. de Bont, Corn fiber, cobs and stover:
354 Enzyme-aided saccharification and co-fermentation after dilute acid pretreatment,
355 Bioresour. Technol. 102 (2011) 5995–6004.
356 [10] Y. Chen, B. Dong, W. Qin, D. Xiao, Xylose and cellulose fractionation from
357 corncob with three different strategies and separate fermentation of them to
358 bioethanol, Bioresour. Technol. 101 (2010) 6994–6999.
359 [11] S. Kumar, Y.S. Negi, J.S. Upadhyaya, Studies on characterization of corn cob
360 based nanoparticles, Adv. Mater. Lett. 1 (2010) 246–253.
361 [12] M. Li, Y.L. Cheng, N. Fu, D. Li, B. Adhikari, X.D. Chen, Isolation and

362 characterization of corncob cellulose fibers using microwave-assisted chemical
363 treatments, Int. J. Food Eng. 10 (2014) 427–436.
364 [13] R.L. Shogren, S.C. Peterson, K.O. Evans, J.A. Kenar, Preparation and
365 characterization of cellulose gels from corn cobs, Carbohydr. Polym. 86 (2011)
366 1351–1357.
367 [14] J. Clever, A. Anderson-specher, J. Jiang, China - Peoples republic of biofuels
368 annual China's 2014 fuel ethanol production is forecast to increase six percent,
369 USDA Foreign Agricutural Serv. (2014).
370 [15] H. Rabemanolontsoa, S. Saka, Comparative study on chemical composition of
371 various biomass species, RSC Adv. 3 (2013) 3946-3956.
372 [16] F.E.M. Van Dongen, D. Van Eylen, M.A. Kabel, Characterization of substituents
373 in xylans from corn cobs and stover, Carbohydr. Polym. 86 (2011) 722–731.
374 [17] Z. Hromádková, J. Kováčiková, A. Ebringerová, Study of the classical and
375 ultrasound-assisted extraction of the corn cob xylan, Ind. Crops Prod. 9 (1999)
376 101–109.
377 [18] E. Lathrop, J. Shollenberger, Corn cobs - their composition, availability, farm and

industrial uses, Illinois, (1947).

[19] G.M. Barton, Definition of biomass samples involving wood, bark and foliage, Biomass 4 (1984) 311-314.

[20] H. Rabemanolontsoa, S. Ayada, S. Saka, Quantitative method applicable for various biomass species to determine their chemical composition, Biomass and Bioenergy. 35 (2011) 4630–4635.

[21] L.E. Wise, M. Maxine, A.A. D'Addieco, Chlorite holocellulose, its fractionation and bearing on summative wood analysis and on studies on the hemicelluloses, Tech. Assoc. Pulp Pap. Ind. 29 (1946) 210–218.

[22] L. Segal, J.J. Creely, A.E. Martin, C.M. Conrad, An empirical method for estimating the degree of crystallinity of native cellulose using the X-ray diffractometer, Text. Res. J. 29 (1959) 786–794.

[23] F. Bertaud, A. Sundberg, B. Holmbom, Evaluation of acid methanolysis for analysis of wood hemicelluloses and pectins, Carbohydr. Polym. 48 (2002) 319–324.

[24] C.W. Dence, The Determination of Lignin, in: S.Y. Lin, C.W. Dence (Eds.),

394 Methods in Lignin Chemistry, Springer Verlag, Berlin, 1992, pp. 33–58.

395 [25] C.-L. Chen, Nitrobenzene and cupric oxide oxidations, in: S.Y. Lin, C.W. Dence

396 (Eds.), Methods in Lignin Chemistry, Springer Verlag, Berlin, 1992, pp. 301–321.

397 [26] E. Allerdings, J. Ralph, H. Steinhart, M. Bunzel, Isolation and structural

398 identification of complex feruloylated heteroxylan side-chains from maize bran,

399 Phytochemistry. 67 (2006) 1276–1286.

400 [27] C.B. Faulds, G. Williamson, The role of hydroxycinnamates in the plant cell wall,

401 J. Sci. Food Agric. 79 (1999) 393–395.

402 [28] T. Ishii, Structure and functions of feruloylated polysaccharides, Plant Sci. 127

403 (1997) 111–127.

404 [29] T.W. Jeffries, Biodegradation of lignin and hemicelluloses, in: C. Ratledge (Ed.),

405 Biochem. Microb. Degrad., Springer Netherlands, Netherlands, 1994, pp. 233–277.

406 [30] J. Grabber, S. Quideau, J. Ralph, *p*-Coumaroyrated syringyl units in maize lignin:

407 Implications for β-ether cleavage by thioacidolysis, Phytochem. 43 (1996) 1189–

408 1194.

409 [31] P. Torre, B. Aliakbarian, B. Rivas, J.M. Dominguez, A. Converti, Release of

ferulic acid from corn cobs by alkaline hydrolysis, Biochem. Eng. J. 40 (2008) 500–506.

[32] M. Takada, S. Saka, Characterization of lignin-derived products from Japanese cedar as treated by semi-flow hot-compressed water, J. Wood Sci. 61 (2015) 299–307.

[33] M. Takada, S. Saka, Comparative study on topochemistry of delignification from Japanese cedar and Japanese beech by hydrothermal treatment, J. Wood Sci. 61 (2015) 602–607.

[34] T. Higuchi, Y. Ito, M. Shimada, I. Kawamura, Chemical properties of milled wood lignin of grasses, Phytochemistry. 6 (1967) 1551–1556.

[35] B.J. Fergus, D.A.I. Goring, The location of guaiacyl and syringyl lignins in birch xylem tissue, Holzforschung. 24 (1970) 113–117.

[36] B.J. Fergus, A.R. Procter, J.A.N. Scott, D.A.I. Goring, The distribution of lignin in sprucewood as determined by ultraviolet microscopy, Wood Sci. Technol. 3 (1969) 117–138.

[37] L. He, N. Terashima, Formation and structure of lignin in monototyledons II.

Deposition and distribution of phenolic acids and their association with cell wall polymers in rice plants (*Oryza sativa*), Mokuzaigakkaishi. 35 (1989) 123–129.

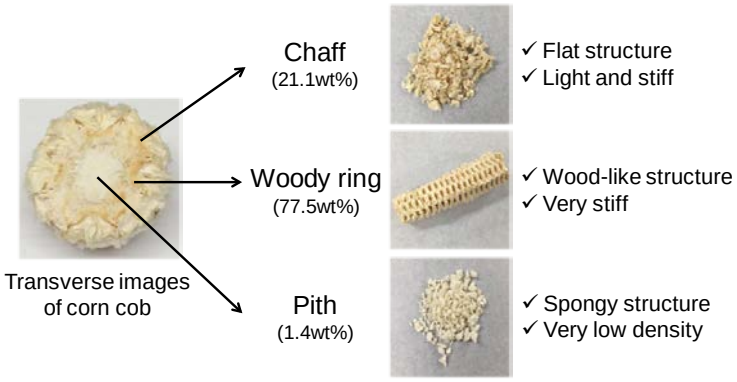

Fig. 1 Three tissue fractions of corn cob

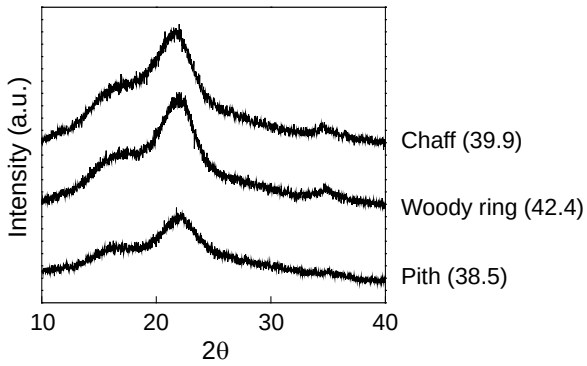

Fig. 2 XRD spectra of three tissue fractions of corn cob. The numbers in parenthesis indicate the crystallinity indexes.

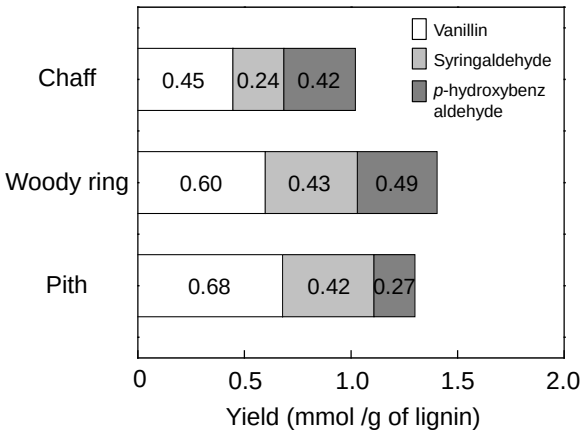

437

438 Fig. 3 Yield of alkaline nitrobenzene oxidation products for three tissue fractions of corn

439 cob

440

441

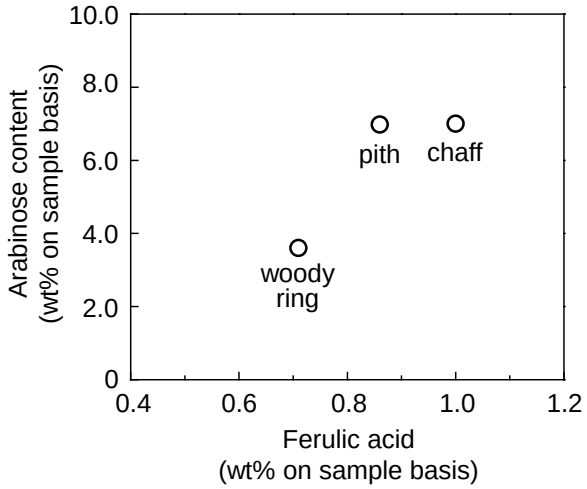

442

443 Fig. 4 Correlation between ferulic acid and arabinose contents in three tissue fractions of

444 corn cob

445

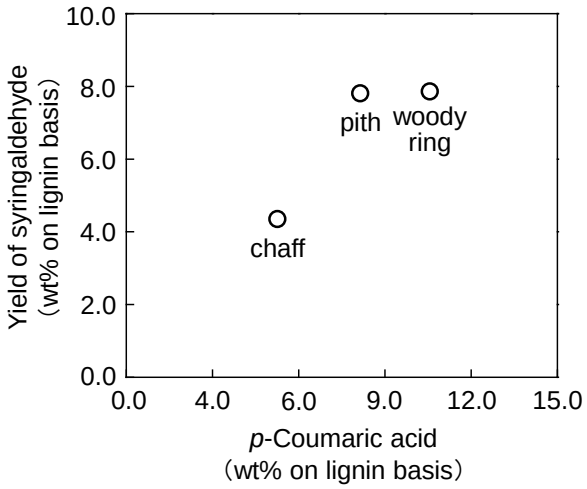

Fig. 5 Correlation between *p*-coumaric acid and the yield of syringaldehyde obtained by alkaline nitrobenzene oxidation in three tissue fractions of corn cob

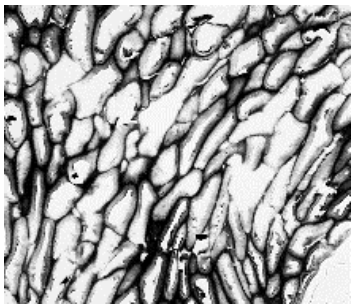

(a) Chaff

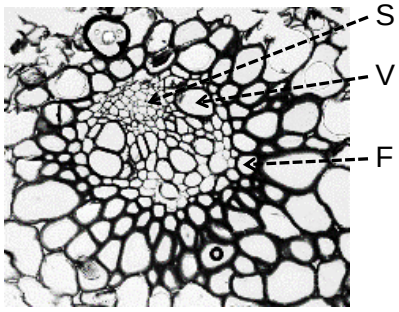

(b-1) Woody ring
(Vascular bundle)

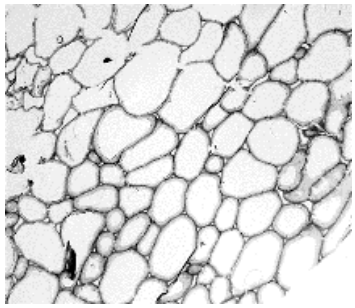

(b-2) Woody ring
(Parenchyma)

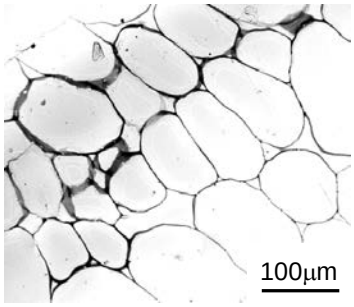

(c) Pith

Fig. 6 UV micrographs of three tissue fractions at a wavelength of 280 nm. S: sieve tube, V: vessel, F: fiber

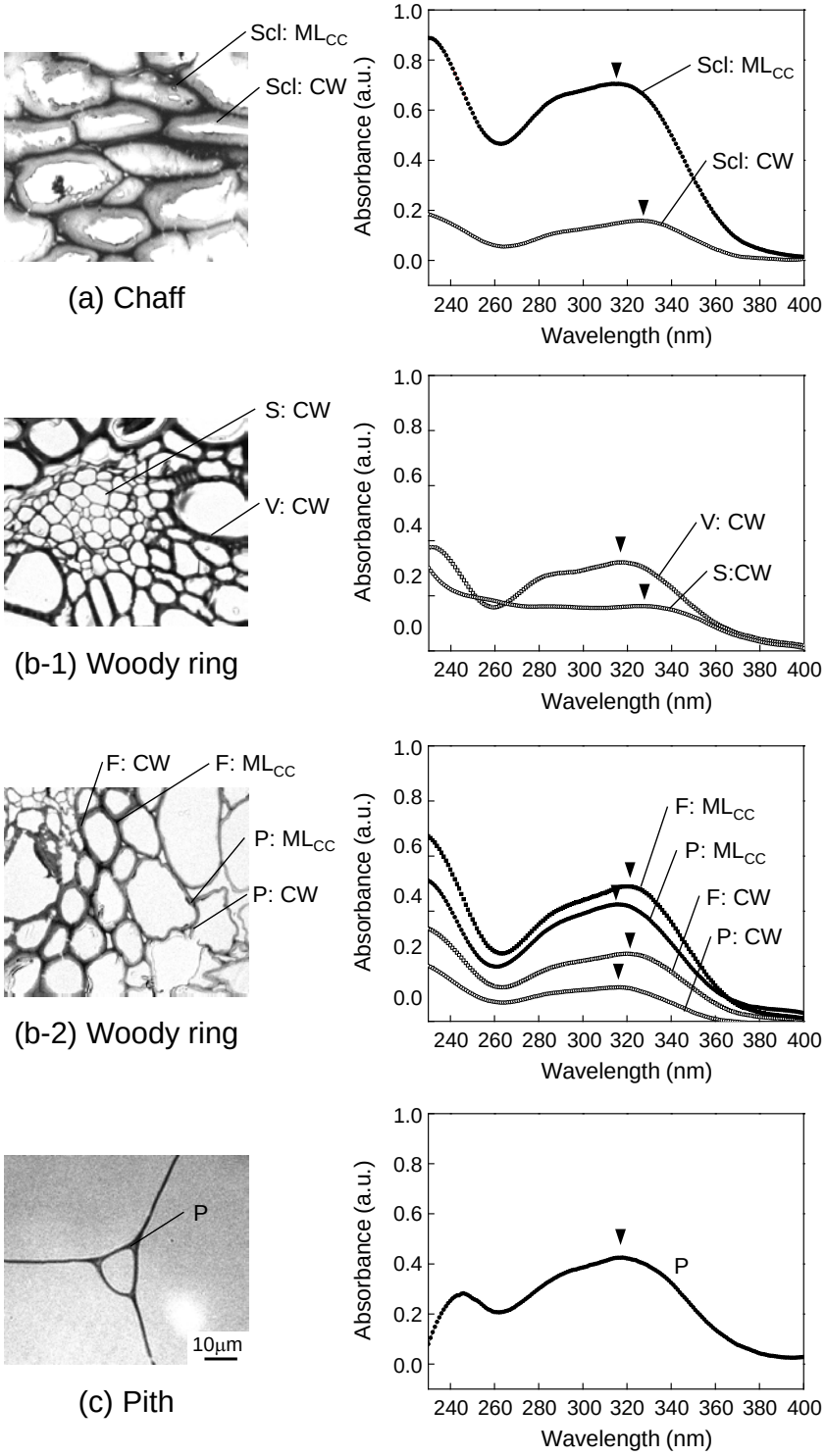

Fig. 7 UV micrographs of three tissue fractions taken at a wavelength of 280 nm and the UV spectra of the morphological regions in three tissue fractions. Scl: sclerenchyma, V: vessel, S: sieve tube, F: fiber, P: parenchyma, CW: cell wall, ML_{CC}: middle lamella at a cell corner